Remediation of bio-refinery wastewater containing organic and inorganic toxic pollutants by adsorption onto chitosan-based magnetic nanosorbent

Abiram Karanam Rathan Kumar, Kongkona Saikia, Gerard Neeraj, Hubert Cabana and Vaidyanathan Vinoth Kumar

ABSTRACT

The novelty of the current study deals with the application of magnetic nanosorbent, chitosan-coated magnetic nanoparticles (cMNPs), to be utilized for the management of lignocellulosic bio-refinery wastewater (LBW) containing three heavy metals and 26 phenolic compounds. The magnetic property of the adsorbent, confirmed by elemental and vibrating sample magnetometer analysis (saturation magnetization of 26.96 emu/g), allows easy separation of the particles in the presence of an external magnetic field. At pH 6.0, with optimized adsorbent dosage of 2.0 g/L and 90 min contact time, maximum removal of phenol (46.2%), copper (42.2%), chromium (18.7%) and arsenic (2.44%) was observed. The extent of removal of phenolic compounds was in the order: polysubstituted > di-substituted > mono-substituted > cresol > phenol. Overall, the adsorption capacity (q_e) of cMNPs varies among the different contaminants in the following manner: copper (1.03 mg/g), chromium (0.20 mg/g), arsenic (0.04 mg/g) and phenol (0.56 mg/g). Post-adsorption, retrieving the cMNPs using an external magnetic field followed by single-step desorption via acid–base treatment is attractive for implementation in industrial settings. Reusability of the adsorbent was studied by recycling the cMNPs for five consecutive rounds of adsorption followed by desorption, at the end of which, cMNPs retained 20% of their initial adsorption capacity.

Key words | bio-refinery wastewater, chitosan magnetic nanoparticle (cMNPs), heavy metals, phenolic compound

Abiram Karanam Rathan Kumar
Kongkona Saikia
Gerard Neeraj
Integrated bioprocessing laboratory, School of Bioengineering,
SRM Institute of Science and Technology,
Kattankulathur, Chennai 603 203,
India

Hubert Cabana (corresponding author)
Laboratoire de génie de l'environnement, Faculté de génie,
Université de Sherbrooke,
2500 boul. de l'Université, Sherbrooke, Québec J1 K 2R1,
Canada
E-mail: *hubert.cabana@usherbrooke.ca*

Vaidyanathan Vinoth Kumar
Department of Biotechnology, School of Bioengineering,
SRM Institute of Science and Technology,
Kattankulathur, Chennai 603203,
India

INTRODUCTION

Bio-refineries employ a third-generation technology which involves the processing of lignocellulosic biomass for production of a wide variety of value-added products and industrial-grade chemicals such as liquid fuels and biodegradable plastics. Bioprocessing of lignocellulosic biomass poses an escalated threat to flora and fauna due to potential release of the accompanying wastewater into the environment. The release of a compendium of toxic pollutants, such as heavy metals, phenols, polycyclic aromatic hydrocarbons, organic compounds of humic origin and acrylic polymers, present at macro (ppm) and micro (ppb) levels, along with a high level of chemical oxygen demand (COD) from wastewater streams, contribute to the complexity in the lignocellulosic bio-refinery wastewater (LBW) treatment process (Pervaiz & Sain 2006; Chen *et al.* 2018).

Generally, the presence of phenolic compounds in LBW can be attributed to the breakdown of lignin in the biomass during the hydrolysis process employed in bio-refinery industries, which can further polymerize to form polyphenols or undergo substitution reactions with nucleophiles (Guerra 2001). Apart from the complexity in biodegradation, these compounds pose acute to chronic hazardous effects

doi: 10.2166/wqrj.2019.003

on living organisms (Guerra 2001; Villegas *et al.* 2016). Phenols exist in common derivative forms, such as bisphenol A (BPA) and chlorophenols, which are proven to be potential endocrine disruptors (Villegas *et al.* 2016; Barrios-Estrada *et al.* 2018). In contrast, the wide applications of Cu, As and Cr containing compounds, like wood preservatives, in the lignocellulosic industries result in the accumulation of these compounds in the generated wastewater, which, in turn, complicates the bioremediation process (Fito *et al.* 2019). Thus, a demand for the treatment of bio-refinery wastewater before release into the environment becomes pivotal (Gang *et al.* 2010).

Technologies which are utilized for the removal of these contaminants include various conventional and advanced methods, like liquid–liquid extraction, adsorption, solid extraction, electrochemical oxidation, Fenton reaction and enzymatic treatments (Villegas *et al.* 2016). Conventionally, adsorption has been a widely utilized technique for the remediation of heavy metals and phenols due to its economic feasibility and ease of operation, along with the regeneration of the adsorbent for future use. However, efficiency of conventional adsorbents is usually limited due to the lack of selectivity, less surface area and slow adsorption kinetics. Thus, nanomaterials are often seen to possess unique size-dependent properties such as high specific surface area and favourable surface chemistry along with the advantages of being highly scaleable and also more amenable to automation (Qu *et al.* 2013; Thekkudan *et al.* 2016). The application of magnetic nanoparticles (MNP) for wastewater treatment is considered a promising practice as they possess enhanced physical properties that improve the overall efficiency of the adsorption process, which in turn, provides a viable solution to the problems encountered in conventional wastewater treatment processes (Qu *et al.* 2013; Thekkudan *et al.* 2016; Li *et al.* 2017). MNPs, when modified using surface engineering techniques, are seen to be more effective adsorbents due to the addition of functional groups that act as active sites for adsorption (Tran *et al.* 2010; Reddy & Lee 2013; Thekkudan *et al.* 2016). An improvement on the use of MNP as adsorbents is the synthesis of chitosan-coated magnetic nanoparticles (cMNPs) that possess both excellent surface adsorption and magnetic properties that facilitate easy separation of these particles after the treatment process (Zhou *et al.* 2009; Qu *et al.* 2013; Thekkudan *et al.* 2016). Chitosan is ideal for such application due to its hydrophobicity, non-toxicity and affinity with various organic molecules and heavy metals owing to the presence of several amino and hydroxyl groups that act as active chelation sites in the polymer matrix (Liu *et al.* 2008; Reddy & Lee 2013). Thus the use of cMNPs overcomes the drawbacks associated with conventional adsorption techniques, such as difficulty in recovery of the adsorbent from the treated wastewater and expenses accrued in regeneration of the saturated adsorbent (Liu *et al.* 2008; Reddy & Lee 2013). Recently, cMNPs have been successfully utilized for the removal of contaminants such as copper (Li *et al.* 2017), chromium (Thinh *et al.* 2013) mercury (Nasirimoghaddam *et al.* 2015), lead and nickel (Tran *et al.* 2010) along with synthetic dye (Hosseini *et al.* 2016) in simulated water or media, which concludes the efficiency of the cMNPs in the remediation of contaminants.

On this basis, the objective of this work was to evaluate the adsorption potential of cMNPs for the constituents of a real-time LBW in which Cu, Cr, As and phenols were identified as the primary contaminants. The synthesized magnetic nanosorbents were characterized using a wide array of particle characterization techniques followed by adsorption studies to optimize the process parameters for the sequestration of contaminants from LBW. To the best of our knowledge, the adsorption process in LBW has not been studied before and this research work is believed to be the first of its kind to employ cMNPs for management of bio-refinery wastewater using adsorption.

MATERIALS AND METHODS

Chemicals

Extra-pure chitosan of medium molecular weight (40 kDa, 75–85% deacetylated) was purchased from Sisco Research Laboratories Pvt. Ltd (TN, India). Reagents for spectrophotometric phenol estimation assay were purchased from Thermo Fisher Scientific Inc. (MA, USA). All other chemicals and reagents utilized in this study were obtained from Sigma Aldrich (MO, USA) and were of analytic grade or better with purity greater than 97%.

Bio-refinery wastewater

The LBW used in the present study was collected from a bio-refinery in Quebec, Canada that produces ethanol and other alternative biofuels. The sampling of the wastewater was done according to *The standard methods for the examination of water and wastewater* (APHA 1989), 1,060B collection of samples and 106 °C sample preservation. For the current experiment, the 'Composite samples' method, specifically multi-subsampling method, was used to collect the samples.

The samples were stored in sterilized glass jars and preserved at 4 °C for further use. The composition of the pH neutralized LBW is presented in Table 1.

Synthesis of chitosan-based magnetic nanosorbent

The protocol for synthesis of cMNPs was previously developed by our research group (Kumar *et al.* 2014; Neeraj *et al.* 2016). The synthesized adsorbent was dried in a hot air oven at 70 °C until it was free of moisture and ground finely using a pestle and mortar. The ground particles were sieved (Tyler Test Sieves, OH, USA) and stored in an airtight container before further use in adsorption studies.

Nanosorbent characterization

Chitosan, MNP and cMNPs were subjected to FTIR analysis (Agilent Technologies, Cary 660 spectrometer, CA, USA) to determine surface functional groups by pulverizing the sample with KBr using a table top hydraulic press to form pellets. Elemental analysis was performed using energy dispersive X-ray spectroscopy (EDAX, FEI Quanta 200 FEG, CA, USA). The shape and structure of MNPs, cMNPs and post-adsorption were studied by subjecting samples to scanning electron microscope analysis (Hitachi S-3000N SEM, Tokyo, Japan). The samples were given a gold–palladium sputter coating and placed on carbon grids for SEM imaging under conditions of high vacuum and 20.0 kV voltage. Thermal properties, changes in physical mass and oxidation of the adsorbent at elevated temperatures were interpreted from thermogravimetric–differential thermal analysis (SetaramSetsys evolution TG-DTA, Caluire, France). A small mass of cMNPs (~50 mg) was heated from 20 °C to 700 °C at an incremental rate of 10 °C per minute in 80% argon atmosphere. The responsiveness of the MNPs and cMNPs under the influence of an external magnetic field was studied by vibrating sample magnetometer (VSM model 7407, Lake Shore Cryotronics Inc., OH, USA) in terms of extent of magnetization (emu/g).

Table 1 | Contaminant profile of LBW, after sludge removal and pH neutralization

Contaminant	(pH 7.0)
Total phenol (mg/L)	2.29 ± 0.83
Copper (mg/L)	4.89 ± 0.42
Chromium (mg/L)	1.87 ± 0.39
Arsenic (mg/L)	2.98 ± 0.06

Batch adsorption experiments

The batch adsorption experiments were performed using 20 mL of LBW in 100 mL conical flasks under varying conditions of contact time, pH and adsorbent dosage. In order to determine the optimum contact time for adsorption, the LBW was supplied with an adsorbent dosage of 2.0 g/L and subjected to controlled orbital shaking at 160 rpm with varying contact time (15–90 min), increasing in 15-min intervals followed by the optimization of pH and adsorbent dosage. Upon completion of the stipulated time for the adsorption process, the cMNPs were separated from the solution by placing neodymium magnets at the bottom of the conical flasks. The adsorbent particles get attracted to the magnet and settle at the surface of the conical flask and the LBW is separated via magnetic decantation to be used for further analysis (Figure 1). Determination of reduction in overall phenolic content in the treated sample was performed by quantification of phenol by AAP method with respect to that of the untreated control sample. The samples were subjected to ICP-MS and GC-MS analysis to estimate the residual concentration of heavy metal and individual phenolic compounds, respectively, post-adsorption. All experiments were performed in triplicate and the mean values of the analysis reported.

The amount of contaminant adsorbed per unit mass of the cMNPs was calculated as the difference of the initial and residual concentration of the substance at equilibrium conditions in the solution using the following mass balance

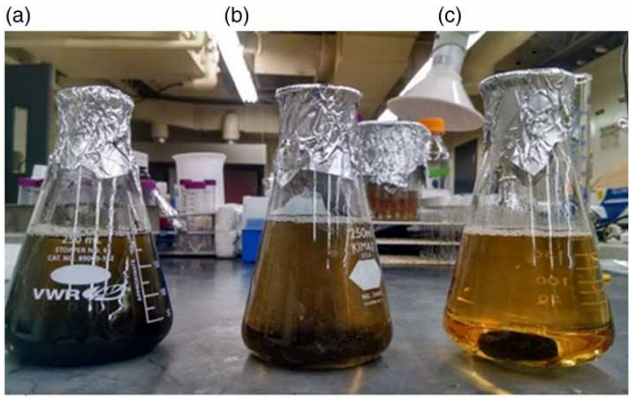

Figure 1 | (a) cMNPs dispersed in LBW; (b) dispersed cMNPs gradually settling under the influence of gravity; (c) rapid settling of dispersed cMNPs upon magnetization by an externally placed magnet at the bottom of the conical flask.

relationship (Kannan & Sundaram 2001; Erdem *et al.* 2004):

$$q_e = (C_o - C_e)\frac{V}{M} \quad (1)$$

$$\%\,\text{Removal} = \frac{(C_o - C_e)}{C_e} \quad (2)$$

where, q_e is the specific adsorption capacity of the adsorbent (mg/g); C_0 (mg/L) and C_e (mg/L) are the initial and equilibrium concentrations of contaminants, respectively; V is the working volume of the wastewater (L); M (g) is the mass of the adsorbent (cMNPs).

Quantification of organic and inorganic contaminants

The LBW samples were subjected to acid digestion prior to ICP-MS analysis for heavy metal analysis, to ensure complete dissolution of the elements to be analysed. Levels of Cu, Cr and As were determined by ICP-MS using a standardized method (US EPA Method-1638 1995) in both treated samples and control wastewater to calculate the removal efficiency of cMNPs for heavy metal removal at varying process parameters.

Estimation of total phenols in the samples was performed using the conventional protocol for phenol quantification using the amino-antipyrine (AAP) method (Dannis 1951). However, due to the inability of this method to detect para-substituted phenols, the samples were subjected to GC-MS analysis, wherein the individual levels of phenolic substituents could be estimated more accurately. The samples for the GC-MS were prepared according to standard protocol established by the Centre of Expertise Environmental Analysis, Quebec, Canada (Özcan *et al.* 2004).

Batch desorption and reusability study

The smart polymer nature of chitosan that allows it to dissociate from MNP under highly acidic conditions and reconstitute with MNP under alkaline conditions to form cMNPs was used for desorption of contaminants (Neeraj *et al.* 2016). cMNPs used earlier for batch adsorption studies were re-suspended in acidified water of pH 2.0 using 1 N HCl at concentration of 2.0 g/L. At highly acidic pH, chitosan gets dissociated from the magnetic support and the solution is subjected to vigorous agitation in an orbital shaker to facilitate maximum desorption. The extent of desorption of phenol and heavy metals was estimated using the corresponding analytical techniques. Reconstitution of cMNPs was carried out by the addition of 1 N NaOH to bring the pH back to 8.0, at which point the dissociated chitosan entraps the MNPs. The regenerated cMNPs were used for five subsequent rounds of adsorption experiments by recycling the same batch of adsorbent via acid–base regeneration, until its adsorption potential had exhausted.

RESULTS AND DISCUSSION

Characterization of magnetic nanosorbent

Thermogravimetric analysis

cMNPs were subjected to TG-DTA and the amount of chitosan in it was estimated. For cMNPs, the initial weight loss of 1.15% observed over the range of 20–101 °C could be attributed to evaporation of moisture present in the cMNPs (Figure 2). The weight loss in nanocomposites is relatively low at temperatures close to 300 °C, primarily due to loss of physical and chemical water from the adsorbent (Li *et al.* 2008). However, at higher temperatures, the weight loss becomes significant, nearly 42%, when the temperature is raised (100–700 °C). The heat flow pattern in cMNPs is rather erratic in comparison to MNP, resulting from varied

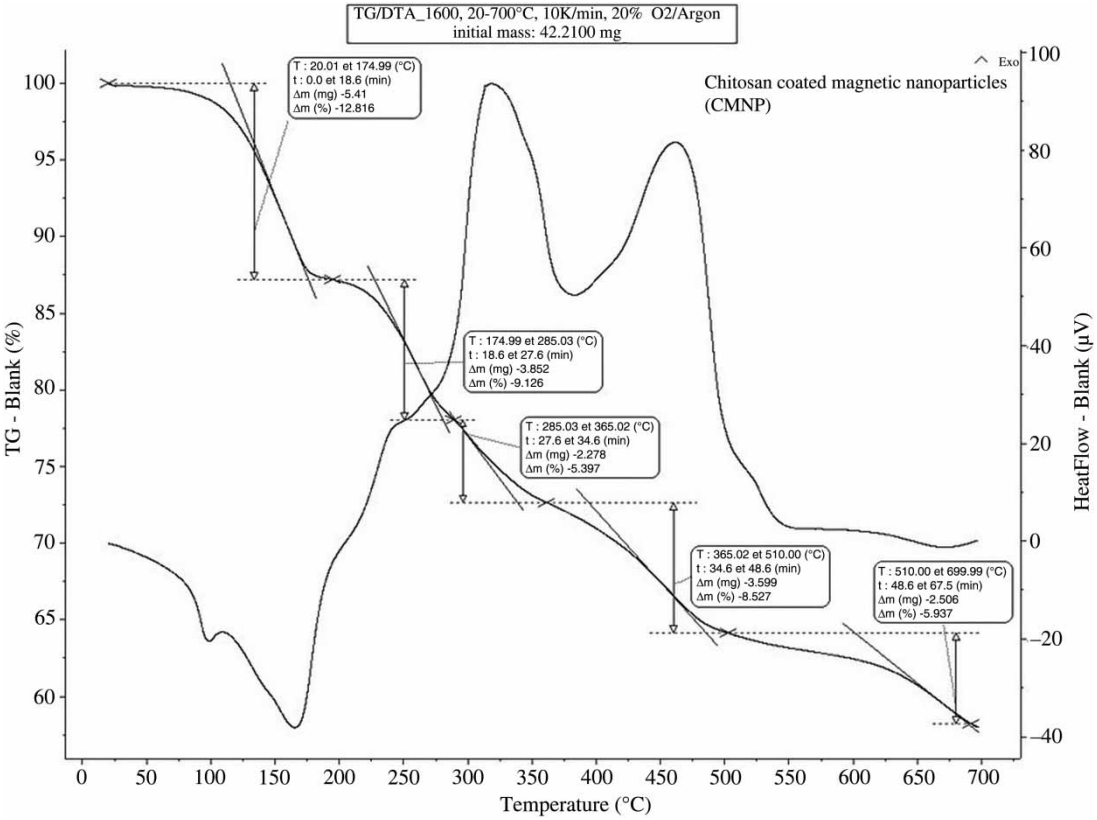

Figure 2 | TG-DTA analysis of cMNPs.

stages of oxidation and combustion of cMNPs, followed by complete destruction of chitosan, leaving residual MNP.

Elemental analysis

The elemental composition of the adsorbent before and after adsorption was evaluated using EDX analysis (Figure 3).

The primary elements present in cMNPs were found to be iron, oxygen and carbon, the presence of which is explained by the coating of the carbonaceous polysaccharide chitosan over the surface of MNP. Another element of significance observed in the analysis is nitrogen, present in the –NH2 groups of the glucosamine repeating units of chitosan (Li *et al.* 2008). Elemental analysis of cMNPs after being

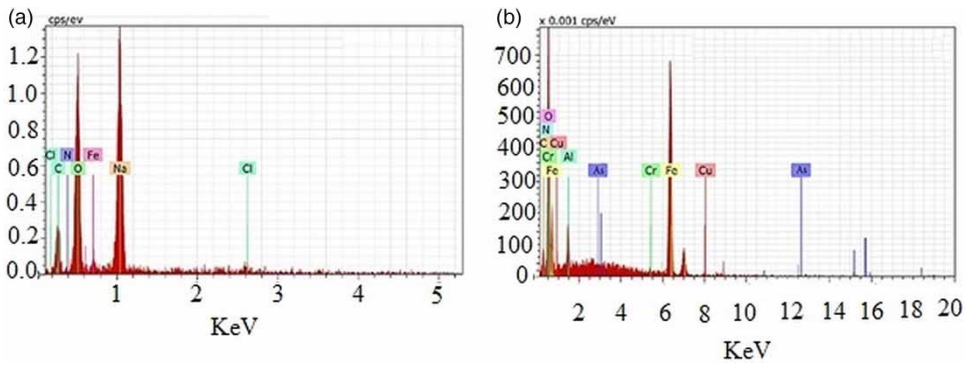

Figure 3 | EDX analysis of (a) cMNPs and (b) cMNPs post-wastewater adsorption treatment.

used for adsorption revealed the presence of heavy metals with copper being adsorbed the most, followed by chromium and arsenic the least. The two different peaks for As and Cr could be attributed to the different ionic states of the metals, As(III) and As(V) and Cr(III) and Cr(VI), respectively. Also, a marked increase in the carbon content after treatment supports the phenomenon of adsorption of phenolic compounds.

Surface functional group analysis

Surface functional groups that could aid the adsorption process via formation of stable attractive forces between the adsorbent and adsorbates were studied using FTIR analysis (Figure 4). From the spectra obtained for cMNPs, the most momentous peak was observed at around 3,440 cm^{-1}, resulting from stretching of the –OH group. The intensity of the peak reflects the relative abundance of the free –OH group. The peak at 600 ± 15 cm^{-1} corresponding to Fe-O bond stretching due to the presence of Fe_3O_4 core confirms the presence of magnetite in the cMNPs (Reddy & Lee 2013). The peaks around $1{,}615 \pm 30$ cm^{-1} are due to the scissoring effect of NH_2 groups. The peak at 1,570 cm^{-1} corresponds to bending of the –N-H bond of primary amine groups. The peak at 770 cm^{-1} and 1,456 cm^{-1} observed for cMNPs corresponds to the rocking and bending effect, respectively, of the –C-H bond of alkyl groups. The peaks observed at 1,414 cm^{-1} and 1,456 cm^{-1} can be attributed to the stretching of the –C-O bond and bending of –OH of primary alcoholic groups present in chitosan (Rinaudo 2006). The minor peak at 1,156 cm^{-1} is seen due to C-N stretch in chitosan (Tran *et al.* 2010). The major flattening of the peak corresponding to hydroxyl groups around 3,440 cm^{-1} in cMNPs after adsorption indicates that this is one of the major functional groups present in the active sites on the adsorbent surface for adsorption. The disappearance of the peak around 1,570 cm^{-1} corresponding to the free amine group in cMNPs after being subjected to wastewater treatment displays the major role played by protonated free amine groups in adsorption. The relative loss of peaks in the $1{,}400 \pm 50$ cm^{-1} region of the spectrum further elucidates the contribution of amine groups in

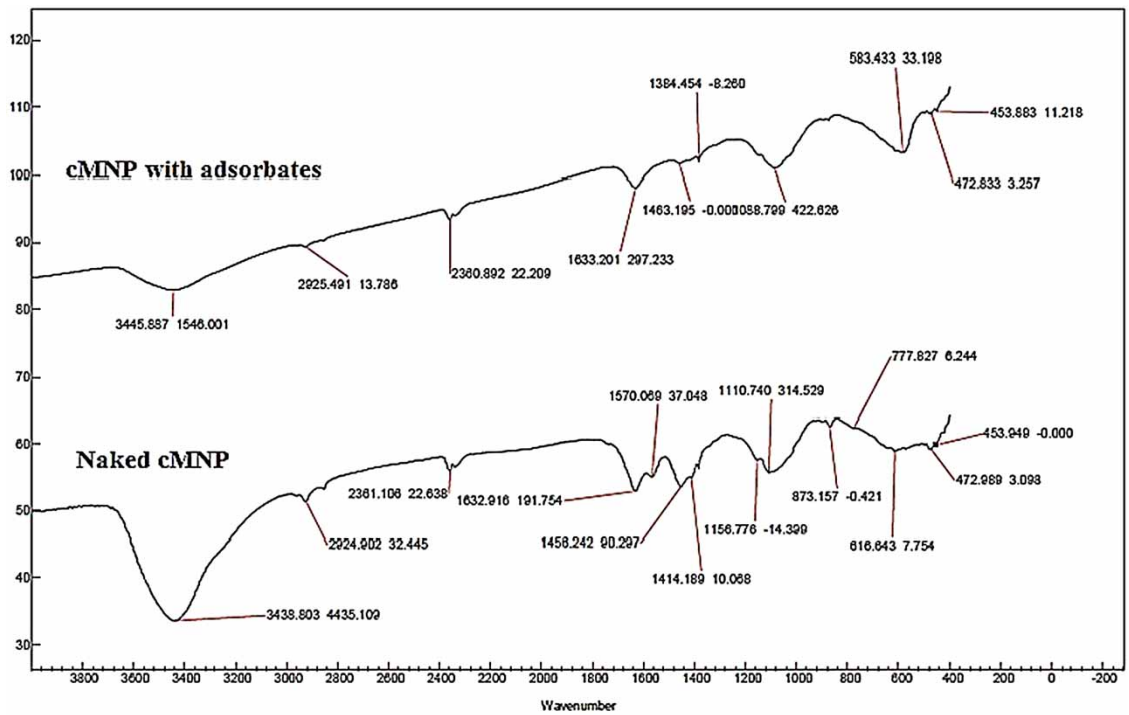

Figure 4 | FTIR analysis of cMNPs before and after adsorption.

chitosan towards its adsorption capability. The peaks observed at 1,463 cm^{-1} and 1,384 cm^{-1} in cMNPs after adsorption arises due to C–N stretch and in ring C–C stretch, specific to aromatic compounds, which confirms the adsorption of phenol and other substituted phenolic compounds (Monier *et al.* 2010). Thus, from the FTIR spectra, the presence of various ionizable surface functional groups such as –OH, –NH2 and –COOH in cMNPs can be inferred, which facilitate ionic interactions with the adsorbate. Further, the adsorptive potential of cMNPs could be explained based on the active surface functional groups, most of which obtain a polycationic state under acidic conditions, thereby stabilizing non-covalent interactions between cMNPs, heavy metals and phenolic compounds.

Magnetization of cMNPs in an external magnetic field

The response of magnetic particles to an external magnetic field is evaluated using VSM analysis in terms of its saturation magnetization (Ms), commonly known as extent of magnetization. It is a relative measure of the magnetic strength of a substance and can be used to predict the magnetic nature of materials in terms of their retentivity and coercivity (Neeraj *et al.* 2016). In this study, it was imperative that we performed VSM analysis to estimate the extent of magnetization of the synthesized magnetic nanosorbent (cMNPs) to confirm their degree of attraction towards a magnet and the magnitude by which their magnetization is affected after adsorption of multiple contaminants. cMNPs possessed a saturation magnetization of 26.96 emu/g, which is quite high considering the fact that they were prepared under laboratory conditions (Figure 5(a)). cMNPs used for adsorption held a saturation magnetization of 21.66 emu/g, which is sufficiently high to separate the adsorbent after completion of the treatment process by the application of a magnetic field using a magnet (Figure 5(b)). The marked decrease in the extent of magnetization of the loaded adsorbent is due to the uptake of several heavy metals and carbonaceous contaminants that tend to reduce the overall magnetization of cMNPs after adsorption. However, the cMNPs still exhibited strong attraction to the magnet even after the adsorption process (Figure 1).

Scanning electron microscopy

The size, shape and surface morphology of cMNPs was determined using SEM. cMNPs possess a uniform and ordered crystalline structure (Figure 6(a)). The shape of the nanoadsorbent was bi-pyramidal in structure and homogenous for all the crystals. cMNPs after adsorption treatment appear different with substantial changes in the surface morphology (Figure 6(b)). The surface appears extensively grainy with no well-defined crystalline structure, in contrast to the unused cMNPs, which possess a smoother surface. The region of white flares in the saturated cMNPs (Figure 6(b)) could possibly be due to adsorption of heavy metals as salts on the surface (Monier *et al.* 2010). Regenerated cMNPs after the acid–base treatment re-attain their crystalline structure (Figure 6(c)). However, a certain degree of loss in the surface homogeneity is observed. Also, the regenerated cMNPs tend to be more aggregated than before due to contact with aqueous environments

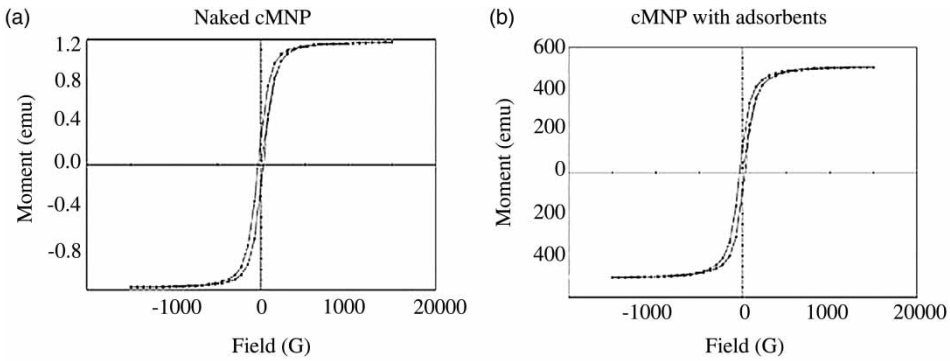

Figure 5 | VSM of (a) cMNPs and (b) after adsorption.

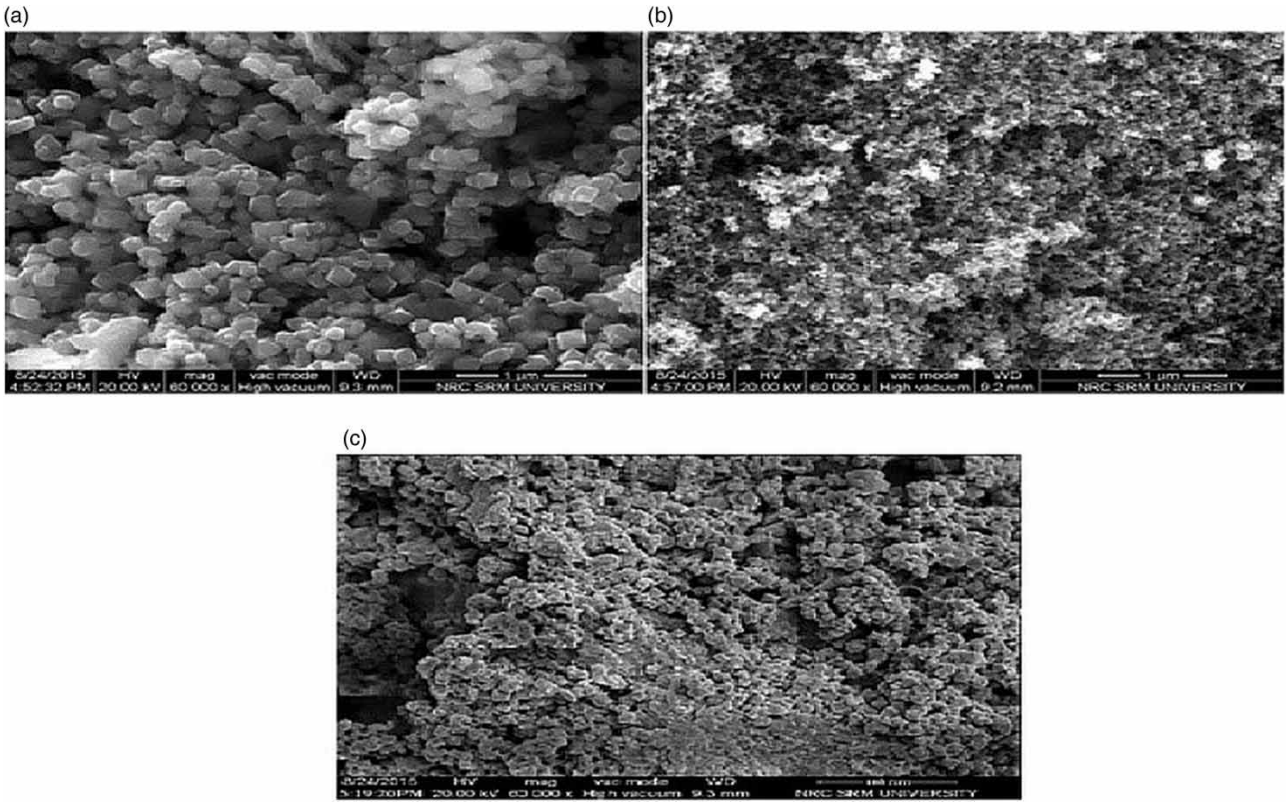

Figure 6 | SEM image of (a) cMNPs; (b) cMNPs post-wastewater adsorption treatment; (c) regenerated cMNPs after adsorption.

which is brought about by random dissociation of chitosan during acid treatment followed by re-adhesion of chitosan upon the addition of the base during regeneration.

Optimization of adsorption conditions for the removal of priority pollutants

Effect of contact time

The contact time between the sorbents and the wastewater is an important parameter that affects the adsorption process. As seen in Figure 7(a), the removal of the heavy metals occurs in the order of Cu > Cr > As with removal of about 50%, 15% and 2%, respectively, after a contact time of 45 min. The multiple adsorption process effected a minimal removal efficiency of As compared to Cu and the variation in contact time did not result in much of a difference in the removal efficiency of As under the tested conditions. The faster rate of adsorption of Cu in comparison to Cr and As could be explained by the interplay of electronegativity, ionic radii, valence state and speciation for preferential adsorption of the heavy metals by chitosan. Speciation of As and Cr in aqueous solution ($Cr_2O_7^{2-}$, CrO_4^{2-}, $H_2AsO_4^-$ and $HAsO_4^{2-}$) effectively increases their ionic radii, which does not favour their adsorption due to decreased mobility in aqueous solution (Sharma *et al.* 2009; Qu *et al.* 2013). The high adsorption for Cu may also be attributed to selectivity of chitosan for this metal (Neeraj *et al.* 2016). Phenols exhibited an increase in the adsorption with time and which was about 40–50% for variation in contact time of 30 min to 90 min, respectively. The competitive adsorption process can be considered to be most effective at contact time of 90 min to achieve maximum removal of all pollutants. However, saturation of the adsorbent occurs at 45 min, evident from the marginal increase in the removal efficiencies after 45 min. The efficiency of the simultaneous adsorption of multiple metals along with the phenols is possible owing to the surface functionality, quantity of surface charge, competitive adsorption affinity of these pollutants for chitosan and the presence of

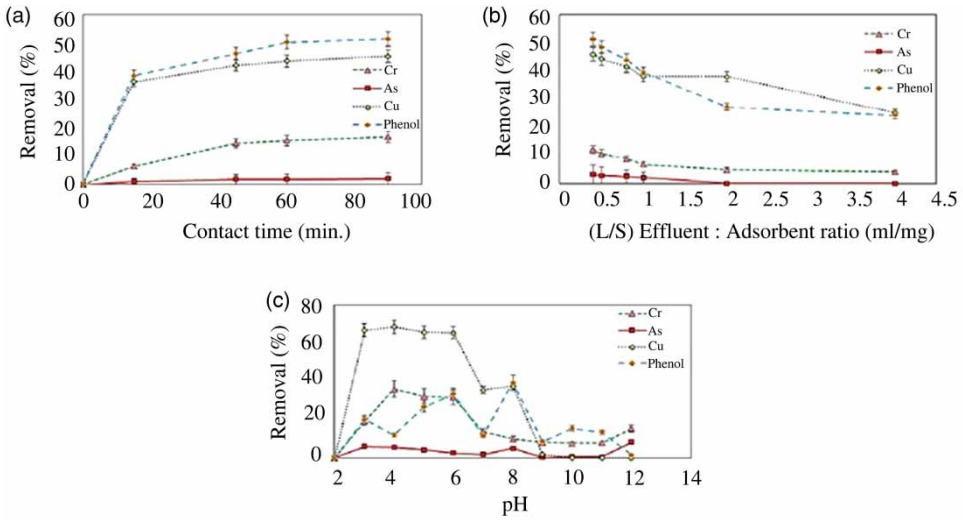

Figure 7 | Effect of (a) contact time (at pH 6.0 and L/S ratio of 0.5 mL/mg); (b) varying adsorbent (L/S ratio) loading (at pH 6.0 and contact time of 60 min); (c) pH (L/S ratio of 0.5 mL/mg and contact time of 60 min) on removal of heavy metals and phenols present in the bio-refinery wastewater. The experiments were performed in triplicate and the mean values have been reported with ± standard deviation.

large numbers of free and accessible active surface sites on the cMNPs (Swayampakula *et al.* 2009).

Effect of adsorbent dosage (liquid: solid loading)

The extent of adsorption from solution is highly influenced by the quantity of adsorbent used. The adsorption of the different pollutants onto the cMNPs increased as the adsorbent dosage was increased. Among the heavy metals studied, Cu was removed to the maximum extent with removal increasing to about 50% as the dosage was increased up to 2.5 g/L (L/S ratio of 0.4), while Cr and As were adsorbed to a lower extent, resulting in removal of about 10% (Figure 7(b)). The extent of removal of phenols was restricted to moderate levels comparable with Cu and showed a similar gradual increase in removal to about 50%, as the adsorbent dosage was increased. It can be observed that the increase in the total number of available active sites on the surface of the cMNPs with increase in adsorbent dosage (at lower L/S ratios) drives a greater removal of the pollutants.

Effect of pH

Among the various parameters involved in the adsorption process, the concentration of protons in the wastewater is seen to have a considerable impact on the adsorption mechanism. The maximal adsorption of the heavy metals (Cu – 80%, Cr – 40%, As – 25%) was seen to occur at pH 4.0 while the mildly acidic pH 6.0 supported the high removal of phenols, followed by a decrease at higher pH values (Figure 7(c)). Highly alkaline conditions having pH greater than 10.0 resulted in minimalistic adsorption of Cu as a repercussion of the inactivity of the surface-active sites on the cMNPs. cMNPs can be subjected to change in the surface charge and zeta potential based on how the solution pH varies with respect to the isoelectric point (pI) of chitosan, which is 6.8 (Reddy & Lee 2013). Under pH conditions lower than 6.8, the protonation of the surface amine groups of chitosan is favoured, which is responsible for the attractive electrostatic interactions between the heavy metals and the cMNPs (Saifuddin & Kumaran 2005). The Cu cations are adsorbed with high specific affinities compared to the other metals. Under highly acidic conditions of pH less than 2.0, the chitosan undergoes dissociation while at highly alkaline conditions, the precipitation of Cu hydroxide occurs which hinders and decreases the adsorption efficiency (Saifuddin & Kumaran 2005). In the case of metals such as Cr and As, these metals exist as anions in solution based on the pH. Hence, at acidic pH conditions less than the isoelectric point (6.8) of chitosan, the adsorbents have a positive surface charge which enables the attraction and adsorption of the metal ions. The stable anions of Cr such as $Cr_2O_7^{2-}$,

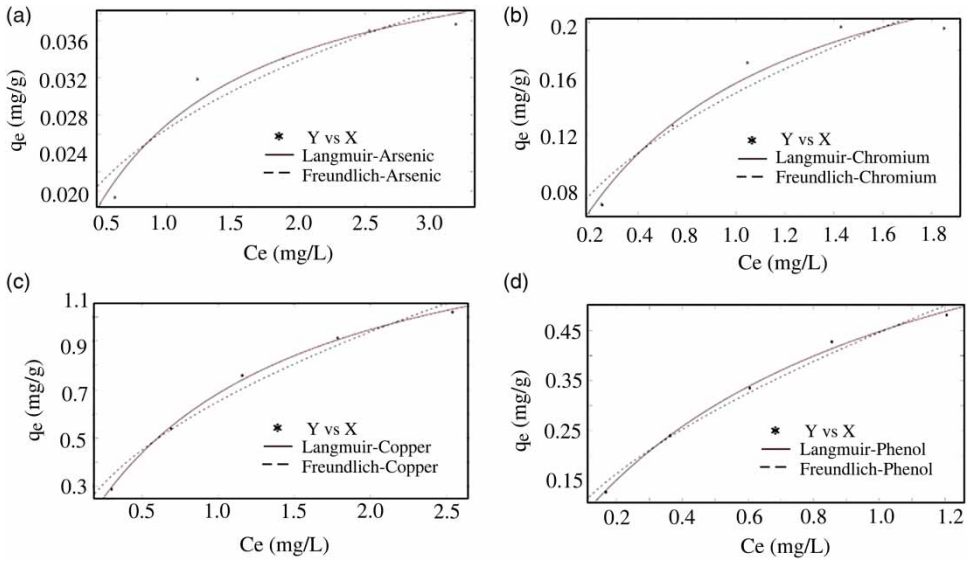

Figure 8 | Langmuir and Freundlich isotherms for adsorption of (a) As, (b) Cr, (c) Cu and (d) phenols.

$HCrO_4^-$, CrO_4^{2-}, $HCr_2O_7^-$ and those of As such as $H_2AsO_4^-$ and $HAsO_4^{2-}$, at pH less than the pI, therefore get adsorbed due to interaction with protonated amine groups on the adsorbent surface (Schmuhl *et al.* 2001). Under alkaline conditions, the presence of hydroxyl groups on the surface of chitosan leads to a repulsion effect between the adsorbent and the anions leading to the decrease in the adsorption efficiency and removal (Li *et al.* 2008). A high binding specificity of chitosan is seen towards Cu compared to that of As and Cr. This lower adsorption of Cr may be attributed to the fact that Cr exists in different valent forms in aqueous solutions, where pH affects the speciation of the metal ion and thus, the stability of these forms along with the surface charge of the adsorbent (Gupta *et al.* 2013).

Studies related to phenolic compounds have shown that the phenols have pKa values ranging from 7.2 to 16.0 depending on their ring substitution at 30 °C. When the pH of the solution exceeds the pKa value, the existence of negatively charged phenolate ions occurs, which otherwise are uncharged molecules below their pKa value. Therefore, uncharged phenols would be adsorbed onto cMNPs at the optimum pH condition, and not phenolate anions which would only exist at pH greater than 9.89. Since the phenols are not in an ionic state at pH 6.0, it is possible that they are adsorbed onto cMNPs via chemical molecular interactions such as covalent bonding.

Equilibrium adsorption isotherms

Isotherms for an adsorption process are vital to predict the degree of accumulation of an adsorbate species on the adsorbent and the relative affinity of the adsorbent for the adsorbate. The extent of adsorption and its possible mechanism were evaluated by the following adsorption isotherms (Figure 8). All isotherms were plotted based on equilibrium conditions achieved at 45 min.

Langmuir isotherm

Equation (3) represents the Langmuir isotherm (Desta 2013):

$$\frac{C_e}{q_e} = \frac{1}{q_m K_L} + \frac{C_e}{q_m} \tag{3}$$

where, q_m is the maximum monolayer adsorption capacity (mg/g) and K_L is the Langmuir constant related to energy

Table 2 | Removal of contaminants from LBW at pH 6.0, adsorbent dosage of 2.0 g/L and at equilibrium contact time of 45 min

Contaminant	q_m (mg/g)	Removal (%)
Arsenic	0.04 ± 0.3	2.44 ± 0.14
Copper	1.03 ± 0.1	42.2 ± 0.19
Chromium	0.20 ± 0.01	18.7 ± 0.111
Phenol	0.56 ± 0.073	46.2 ± 0.39

Table 3 | Adsorption isotherm parameters for As (arsenic), Cr (chromium), Cu (copper) and phenols' adsorption

	Langmuir isotherm			Freundlich isotherm		
Contaminants	q_m(mg/g)	K_L(L/mg)	R^2	K_F ((mg/g)(L/mg)$^{(1/n)}$)	n_f (g/L)	R^2
As	0.048	1.258	0.955	0.0265	2.851	0.888
Cr	0.2977	1.3870	0.970	0.1668	2.05	0.917
Cu	1.5420	0.7972	0.998	0.6504	1.892	0.974
Phenols	0.8830	1.0310	0.997	0.4462	1.605	0.983

of adsorption (L/mg). The Langmuir isotherm assumes a homogenous monolayer adsorption, without considering any interactions between the adsorbate species. The maximum monolayer adsorption capacity per gram of cMNPs, according to the Langmuir isotherm at equilibrium conditions, was found to be 0.048 mg of As, 0.2977 mg of Cr, 1.542 mg of Cu and 0.883 mg of phenol. The experimentally determined adsorption capacities of cMNPs for these contaminants is shown in Table 2.

Freundlich isotherm

Equation (4) represents the mathematical expression of the Freundlich isotherm (Desta 2013):

$$log(q_e) = log(K_F) + \frac{1}{n_f}\, log(C_e) \tag{4}$$

where, K_F ((mg/g) (L/mg)$^{(1/n)}$) is the Freundlich constant related to the bonding energy, indicative of the amount of adsorbate sequestered by the adsorbent for unit equilibrium concentration. $1/n_f$ is the heterogeneity factor indicative of the degree of non-linearity of the adsorption process. If n_f (g/L) value is below unity, the process is physisorption and otherwise, chemisorption. The Freundlich model assumes a heterogeneous system where interaction occurs between the adsorbate molecules and occurs in a multilayer fashion over the adsorbent surface. The obtained Freundlich isotherm constant values (n_f) for all adsorbates were greater than unity (Table 3), indicating that adsorption of heavy metals and phenol occurs via chemical interactions with the cMNPs (chemisorption). Figure 8 shows the fit of equilibrium data pertaining to Freundlich and Langmuir isotherms.

The Langmuir isotherm assumes the adsorption of only one metal ion onto the adsorbent's surface, whereas the Freundlich isotherm assumes that heterogeneous surfaces are involved in adsorption. From the adsorption studies, the

Table 4 | Percentage removal of different phenolic compounds from the LBW at pH 6.0, adsorbent dosage of 2.0 g/L and contact time of 45 min

Compound	Initial conc. (µg/L)	Final conc. (µg/L)	Removal (%)
Phenol	8.97	5.12	42.9
o-cresol	3.17	0.76	76.0
m-cresol	1.93	0.55	71.5
p-cresol	2.44	1.02	58.2
2-nitrophenol	1.13	1.00	11.5
2,4-dimethylphenol	0.9	0.5	44.4
2,4-dinitrophenol	0.4	0.275	31.3
4-nitrophenol	3.0	2.0	33.3
2-methyl – 4,6-dinitrophenol	60	10	83.3
3-chlorophenol	0.85	0.50	41.2
4-chlorophenol	0.58	0.50	16.0
2,3-dichlorophenol	1.15	0.50	56.2
2,4 + 2,5-dichlorophenol	0.85	0.50	41.2
2,6-dichlorophenol	0.78	0.50	35.9
3,4-dichlorophenol	2.75	1.50	45.5
3,5-dichlorophenol	1.93	0.50	74.1
2,3,4-trichlorophenol	0.70	0.55	21.4
2,3,5-trichlorophenol	0.75	0.50	33.3
2,3,6-trichlorophenol	1.46	0.86	41.1
2,4,5-trichlorophenol	1.2	0.50	58.3
2,4,6-trichlorophenol	1.23	0.97	21.1
3,4,5-trichlorophenol	0.83	0.50	39.8
2,3,4,5-tetrachlorophenol	0.68	0.50	26.5
2,3,4,6-tetrachlorophenol	539.5	131	75.6

R^2 value for the heavy metals and the phenols in the case of the Langmuir isotherm was found to be higher than that of the Freundlich isotherm which makes the Langmuir isotherm the best fit for the adsorption of the heavy metals and phenolic compounds (Desta 2013; Mohammad *et al.* 2017).

Complete quantitative analysis for specific phenolic compounds

The conventional method of phenol estimation using 4-amino-antipyrine (4-AAP) gives the overall concentration of only certain phenolic substances, such as meta- and ortho-substituted phenols and conjugated phenols. To determine the level of each of these individual phenolic substances, qualitative and quantitative analysis of the treated and untreated samples was performed using GC-MS. The results obtained were quite promising, considering the multi-component nature of the adsorption process. The percentage removals of individual phenolic compounds before and after adsorption are presented in Table 4. Despite the presence of 26 phenolic compounds, most of the toxic pollutants were removed significantly relative to their initial concentrations in the wastewater. The mechanism of interaction between chitosan and phenolic molecules at pH 6.0 is hypothesized to be due to hydrogen bonding and hydrophobic interactions, but not electrostatic interactions (Long *et al.* 2009). Surprisingly, increased removal of substituted phenols was achieved in comparison to generic phenol which can be attributed to greater charge delocalization due to increased π–π electron cloud dispersion forces resulting in a corresponding intensification of the electron density in the basal aromatic plane of the compound that resulted in enhanced adsorption of substituted phenols (Kalkan *et al.* 2012). Lower removal of nitro-phenols was observed, which might be due to lowered affinity of chitosan towards phenols with nitrogen atoms, due to electron withdrawal effect or reduced adsorption due to possible steric effects or molecular sieve effects of the pre-adsorbed metals. Other abnormalities could be due to initial high adsorption at the entrance of the pore, thereby limiting further diffusion of solute molecules (Long *et al.* 2009).

Operational stability of cMNPs

Desorption of the As, Cr and phenol is found to increase with every subsequent cycle which could be due to the cumulative release of adsorbed species from previous rounds of adsorption. Heavy metals show excellent

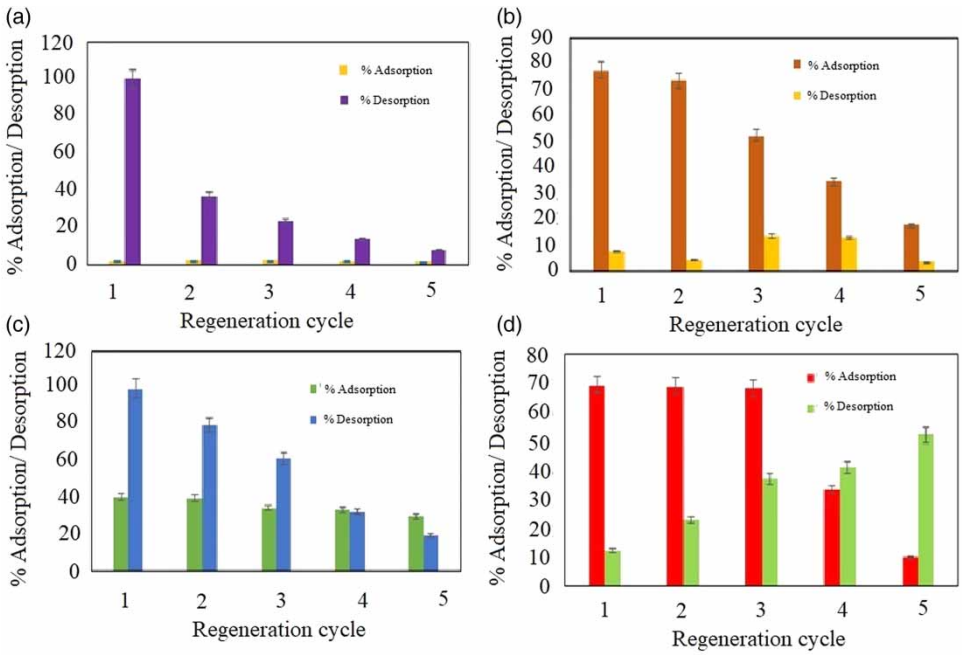

Figure 9 | Reusability study of cMNPs over five consecutive cycles of adsorption of (a) As, (b) Cr, (c) Cu and (d) phenols in LBW and desorption.

Table 5 | Comparison of maximum monolayer adsorption of organic and inorganic pollutants onto various adsorbents

Adsorbent	Heavy metal	q_m (mg/g)	Demerits	References
Zeolite	Cu	1.64	The sensitivity deactivation by irreversible adsorption or steric blockage of secondary products	Erdem *et al.* (2004)
	Cr	0.2		Wang & Peng (2010)
	As	–		
	Phenols	0.87		Yousef *et al.* (2011)
Fly ash	Cu	0.1825	Low adsorption efficiency	Salam *et al.* (2011)
	Cr	0.83		Wang *et al.* (2017)
	As	0.596		Meher *et al.* (2016)
	Phenols	0.06		Potgieter *et al.* (2009)
Rice husk	Cu	1.93	Finite resource and not available universally	Salam *et al.* (2011)
	Cr	0.79		Bishnoi *et al.* (2004)
	As	2.24		Van Dang *et al.* (2009)
	Phenols	0.91		Daffalla *et al.* (2013)
Activated carbon	Cu	0.96	Cost inefficiency and requires complexing agents to improve its removal performance	Tumin *et al.* (2008)
	Cr	0.3–0.4		Pang *et al.* (2015)
	As	0.855		Mohan & Pittman Jr (2007)
	Phenols	1.48		Vázquez *et al.* (2007)
Activated alumina	Cu	–	Requires strong acid or base for regeneration	
	Cr	9.6		Bishnoi *et al.* (2004)
	As	0.180		Norton *et al.* (2001)
	Phenols	–		
MNP	Cu	0.47	Low surface area and less adsorption efficiency	Dada *et al.* (2016)
	Cr	1.2		Parsons *et al.* (2014)
	As	0.3–1.3		Monárrez-Cordero *et al.* (2016)
	Phenols	2.5		Mihoc *et al.* (2014)
cMNPs	Cu	21.5	Simulated water with individual contaminants	Yuwei & Jianlong (2011)
	Cr(VI)	–		
	As	18.4		Anto & Annadurai (2012)
	Phenols	–		
cMNPs	Cu	1.04	–	Current study
	Cr	1.2		
	As	0.04		
	Phenols	0.56		

desorption in the following order: As > Cu > Cr (Figure 9). The high desorption of heavy metals in the first three rounds is a testament to the non-covalent physical adsorption phenomena, involving dipole–dipole and Van der Waals interaction between the nanosorbent and the metal ions. However, the lower desorption of phenol at the end of the fifth cycle in comparison to heavy metals indicates that interactions stronger than non-covalent attraction are at play between the adsorbent and phenolic compounds. By the fifth cycle of reuse, the adsorption potential of the cMNPs had diminished by more than 80% of its initial adsorption capacity for all the adsorbates studied. The recycle phase would essentially employ a magnetic field under which the saturated adsorbent alone would be retained to be subjected to acid–base treatment to facilitate desorption of metals and phenols. Upon completion of desorption, the regenerated adsorbent can be once again recycled into the process stream by relieving the magnetic field. This way, the magnetic nature of the adsorbent can be exploited to design a continuous wastewater treatment methodology which could be scaled up to potential large-scale operations in the bio-refinery industry. In doing so, the reusability of the adsorbent can be prolonged for a greater number of cycles reducing the discrete number of steps required for adsorbent regeneration, while also maximizing the efficiency and economics of the treatment process.

Potential of cMNPs for the treatment of contaminants in wastewater

Recently, the potential of nanotechnology for wastewater treatment was demonstrated at a pilot level for adsorption of the various contaminants by Jassby *et al.* (2018) and Alvarez *et al.* (2018). The comparison of maximum adsorption capacity of the various adsorbents used in their studies for As, Cr, Cu and phenols is given in Table 5. It shows that the cMNPs studied in this present study have greater adsorption capacity for these contaminants.

CONCLUSION

cMNPs are considered the next generation magnetic nano-sorbents that provide a realistic approach in the treatment of LBW by overcoming several demerits of existing adsorbent in terms of feasibility and efficiency. Their easy recovery has resulted in a markedly improved performance in the ternary adsorption process for the removal of multiple pollutants compared to its conventional counterparts. The experiments conducted by varying the contact time, adsorbent dosage and wastewater pH exhibited the increasing removal efficiencies of the heavy metal ions with the removal of copper (42.22%) being the highest and clearly presented the common adsorption affinity rates of phenols at the different conditions and that they occupy the maximal surface areas of the magnetic particles. Reduction in steps involved in unit operations would lower the energy and manual labour requirements of the process, contributing to the economic feasibility, the prime focus for scale up of any technology. The promising characteristics of the cMNPs clearly exhibit their potential, which can be used in idealistic wastewater treatment applications for effective removal of pollutants to low concentrations by competitive adsorption.

ACKNOWLEDGEMENTS

The authors express their deepest gratitude to the financial support extended by Natural Sciences and Engineering Research Council of Canada and SRM Institute of Science and Technology, Chennai, India to facilitate our research. Also, we would like to thank Mr. Olivier Savary and Ms. Irene Kelsey, Sherbrooke University, for their time and help.

REFERENCES

Alvarez, P. J., Chan, C. K., Elimelech, M., Halas, N. J. & Villagrán, D. 2018 Emerging opportunities for nanotechnology to enhance water security. *Nature Nanotechnology* **13** (8), 634–641.

Anto, S. M. & Annadurai, G. 2012 Arsenic adsorption from aqueous solution using chitosan nanoparticle. *Research Journal of Nanoscience and Nanotechnology* **2**, 31–45.

APHA 1989 *Standard Methods for the Examination of Water and Wastewater*, 17th edn. American Public Health Association, Washington, DC, USA.

Barrios-Estrada, C., de Jesús Rostro-Alanis, M., Muñoz-Gutiérrez, B. D., Iqbal, H. M., Kannan, S. & Parra-Saldívar, R. 2018 Emergent contaminants: Endocrine disruptors and their laccase-assisted degradation–a review. *Science of the Total Environment* **612**, 1516–1531.

Bishnoi, N. R., Bajaj, M., Sharma, N. & Gupta, A. 2004 Adsorption of Cr(VI) on activated rice husk carbon and activated alumina. *Bioresource Technology* **91** (3), 305–307.

Chen, P., Anderson, E., Addy, M., Zhang, R., Cheng, Y., Peng, P., Ma, Y., Fan, L., Zhang, Y. & Lu, Q. 2018 Breakthrough technologies for the biorefining of organic solid and liquid wastes. *Engineering* **4** (4), 574–580.

Dada, A. O., Latona, D. F., Ojediran, O. J. & Nath, O. O. 2016 Adsorption of Cu(II) onto bamboo supported manganese (BS-Mn) nanocomposite: Effect of operational parameters, kinetic, isotherms, and thermodynamic studies. *Journal of Applied Sciences and Environmental Management* **20** (2), 409–422.

Daffalla, S. B., Mukhtar, H. & Shaharun, M. S. 2013 Removal of phenol from aqueous solutions using rice husk ash. *Caspian Journal of Applied Sciences Research* **2**, 36–49.

Dannis, M. 1951 Determination of phenols by the amino-antipyrine method. *Sewage and Industrial Wastes* **23** (12), 1516–1522.

Desta, M. B. 2013 Batch sorption experiments: Langmuir and Freundlich isotherm studies for the adsorption of textile metal ions onto teff straw (Eragrostis tef) agricultural waste. *Journal of Thermodynamics* **2013**, 1–4.

Erdem, E., Karapinar, N. & Donat, R. 2004 The removal of heavy metal cations by natural zeolites. *Journal of Colloid and Interface Science* **280** (2), 309–314.

Fito, J., Tefera, N. & Van Hulle, S. W. 2019 Sugarcane biorefineries wastewater: Bioremediation technologies for environmental sustainability. *Chemical and Biological Technologies in Agriculture* **6** (1), 6.

Gang, D. D., Deng, B. & Lin, L. 2010 As(III) removal using an iron-impregnated chitosan sorbent. *Journal of Hazardous Materials* **182** (1–3), 156–161.

Guerra, R. 2001 Ecotoxicological and chemical evaluation of phenolic compounds in industrial effluents. *Chemosphere* **44** (8), 1737–1747.

Gupta, V., Pathania, D., Agarwal, S. & Sharma, S. 2013 Removal of Cr(VI) onto *Ficus carica* biosorbent from water. *Environmental Science and Pollution Research* **20** (4), 2632–2644.

Hosseini, F., Sadighian, S., Hosseini-Monfared, H. & Mahmoodi, N. M. 2016 Dye removal and kinetics of adsorption by magnetic chitosan nanoparticles. *Desalination and Water Treatment* **57** (51), 24378–24386.

Jassby, D., Cath, T. Y. & Buisson, H. 2018 The role of nanotechnology in industrial water treatment. *Nature Nanotechnology* **13** (8), 670–672.

Kalkan, N. A., Aksoy, S., Aksoy, E. A. & Hasirci, N. 2012 Preparation of chitosan-coated magnetite nanoparticles and application for immobilization of laccase. *Journal of Applied Polymer Science* **123** (2), 707–716.

Kannan, N. & Sundaram, M. M. 2001 Kinetics and mechanism of removal of methylene blue by adsorption on various carbons – a comparative study. *Dyes and Pigments* **51** (1), 25–40.

Kumar, V. V., Sivanesan, S. & Cabana, H. 2014 Magnetic cross-linked laccase aggregates – Bioremediation tool for decolorization of distinct classes of recalcitrant dyes. *Science of the Total Environment* **487**, 830–839.

Li, G.-Y., Jiang, Y.-R., Huang, K.-L., Ding, P. & Chen, J. 2008 Preparation and properties of magnetic Fe_3O_4–chitosan nanoparticles. *Journal of Alloys and Compounds* **466** (1–2), 451–456.

Li, J., Jiang, B., Liu, Y., Qiu, C., Hu, J., Qian, G., Guo, W. & Ngo, H. H. 2017 Preparation and adsorption properties of magnetic chitosan composite adsorbent for Cu^{2+} removal. *Journal of Cleaner Production* **158**, 51–58.

Liu, X., Hu, Q., Fang, Z., Zhang, X. & Zhang, B. 2008 Magnetic chitosan nanocomposites: A useful recyclable tool for heavy metal ion removal. *Langmuir* **25** (1), 3–8.

Long, C., Lu, J., Li, A. & Zhang, Q. 2009 Removal of endocrine disrupting chemicals from aqueous phase using spherical microporous carbon prepared from waste polymeric exchanger. *Water Science and Technology* **60** (6), 1607–1614.

Meher, A. K., Das, S., Rayalu, S. & Bansiwal, A. 2016 Enhanced arsenic removal from drinking water by iron-enriched aluminosilicate adsorbent prepared from fly ash. *Desalination and Water Treatment* **57** (44), 20944–20956.

Mihoc, G., Ianoş, R. & Păcurariu, C. 2014 Adsorption of phenol and p-chlorophenol from aqueous solutions by magnetic nanopowder. *Water Science and Technology* **69** (2), 385–391.

Mohammad, M., Yakub, I., Yaakob, Z., Asim, N. & Sopian, K. 2017 Adsorption isotherm of chromium (Vi) into zncl2 impregnated activated carbon derived by jatropha curcas seed hull. *IOP Conference Series: Materials Science and Engineering* **1**, 012013. IOP Publishing.

Mohan, D. & Pittman Jr., C. U. 2007 Arsenic removal from water/wastewater using adsorbents – a critical review. *Journal of Hazardous Materials* **142** (1–2), 1–53.

Monárrez-Cordero, B. E., Amézaga-Madrid, P., Leyva-Porras, C. C., Pizá-Ruiz, P. & Miki-Yoshida, M. 2016 Study of the adsorption of arsenic (III and V) by magnetite nanoparticles synthetized via AACVD. *Materials Research* **19**, 103–112.

Monier, M., Ayad, D., Wei, Y. & Sarhan, A. 2010 Adsorption of Cu(II), Co(II), and Ni(II) ions by modified magnetic chitosan chelating resin. *Journal of Hazardous Materials* **177** (1–3), 962–970.

Nasirimoghaddam, S., Zeinali, S. & Sabbaghi, S. 2015 Chitosan coated magnetic nanoparticles as nano-adsorbent for efficient removal of mercury contents from industrial aqueous and oily samples. *Journal of Industrial and Engineering Chemistry* **27**, 79–87.

Neeraj, G., Krishnan, S., Kumar, P. S., Shriaishvarya, K. R. & Kumar, V. V. 2016 Performance study on sequestration of copper ions from contaminated water using newly synthesized high effective chitosan coated magnetic nanoparticles. *Journal of Molecular Liquids* **214**, 335–346.

Norton, M., Chang, Y., Galeziewski, T., Kommineni, S. & Chowdhury, Z. 2001 Throw-away iron and aluminum sorbents versus conventional activated alumina for arsenic removal – pilot testing results. In: *Proceedings Annual Conference*. American Water Works Association, Washington, DC, USA, pp. 2073–2087.

Özcan, A. S., Erdem, B. & Özcan, A. 2004 Adsorption of acid blue 193 from aqueous solutions onto Na–bentonite and DTMA–bentonite. *Journal of Colloid and Interface Science* **280** (1), 44–54.

Pang, M., Liu, B., Kano, N. & Imaizumi, H. 2015 Adsorption of chromium (VI) onto activated carbon modified with $KMnO_4$. *Journal of Chemistry and Chemical Engineering* **9**, 280–287.

Parsons, J. G., Hernandez, J., Gonzalez, C. M. & Gardea-Torresdey, J. 2014 Sorption of Cr(III) and Cr(VI) to high and low pressure synthetic nano-magnetite (Fe_3O_4) particles. *Chemical Engineering Journal* **254**, 171–180.

Pervaiz, M. & Sain, M. 2006 Biorefinery: opportunities and barriers for petro-chemical industries. *Pulp and Paper Canada* **107** (6), 31–33.

Potgieter, J., Bada, S. & Potgieter-Vermaak, S. 2009 Adsorptive removal of various phenols from water by South African coal fly ash. *Water SA* **35**, 1.

Qu, X., Alvarez, P. J. & Li, Q. 2013 Applications of nanotechnology in water and wastewater treatment. *Water Research* **47** (12), 3931–3946.

Reddy, D. H. K. & Lee, S.-M. 2013 Application of magnetic chitosan composites for the removal of toxic metal and dyes from aqueous solutions. *Advances in Colloid and Interface Science* **201**, 68–93.

Rinaudo, M. 2006 Chitin and chitosan: Properties and applications. *Progress in Polymer Science* **31** (7), 603–632.

Saifuddin, M. & Kumaran, P. 2005 Removal of heavy metal from industrial wastewater using chitosan coated oil palm shell charcoal. *Electronic Journal of Biotechnology* **8** (1), 43–53.

Salam, O. E. A., Reiad, N. A. & ElShafei, M. M. 2011 A study of the removal characteristics of heavy metals from wastewater by low-cost adsorbents. *Journal of Advanced Research* **2** (4), 297–303.

Schmuhl, R., Krieg, H. & Keizer, K. 2001 Adsorption of Cu(II) and Cr(VI) ions by chitosan: Kinetics and equilibrium studies. *Water SA* **27** (1), 1–8.

Sharma, Y., Srivastava, V., Singh, V., Kaul, S. & Weng, C. 2009 Nano-adsorbents for the removal of metallic pollutants from water and wastewater. *Environmental Technology* **30** (6), 583–609.

Swayampakula, K., Boddu, V. M., Nadavala, S. K. & Abburi, K. 2009 Competitive adsorption of Cu(II), Co(II), and Ni(II) from their binary and tertiary aqueous solutions using chitosan-coated perlite beads as biosorbent. *Journal of Hazardous Materials* **170** (2–3), 680–689.

Thekkudan, V. N., Vaidyanathan, V. K., Ponnusamy, S. K., Charles, C., Sundar, S., Vishnu, D., Anbalagan, S., Vaithyanathan, V. K. & Subramanian, S. 2016 Review on nanoadsorbents: A solution for heavy metal removal from wastewater. *IET Nanobiotechnology* **11** (3), 213–224.

Thinh, N. N., Hanh, P. T. B., Hoang, T. V., Hoang, V. D., Dang, L. H., Van Khoi, N. & Dai Lam, T. 2013 Magnetic chitosan nanoparticles for removal of Cr(VI) from aqueous solution. *Materials Science and Engineering: C* **33** (3), 1214–1218.

Tran, H. V., Dai Tran, L. & Nguyen, T. N. 2010 Preparation of chitosan/magnetite composite beads and their application for removal of Pb(II) and Ni(II) from aqueous solution. *Materials Science and Engineering: C* **30** (2), 304–310.

Tumin, N. D., Chuah, A. L., Zawani, Z. & Rashid, S. A. 2008 Adsorption of copper from aqueous solution by Elais Guineensis kernel activated carbon. *Journal of Engineering Science and Technology* **3** (2), 180–189.

US EPA Method 1638 1995 Determination of trace elements in ambient waters by ICP-MS – EPA 821-R-95-031, April 1995.

Van Dang, S., Kawasaki, J., Abella, L. C., Auresenia, J., Habaki, H., Kosuge, H. & Doan, H. T. 2009 Removal of arsenic from simulated groundwater by adsorption using iron-modified rice husk carbon. *Journal of Water and Environment Technology* **7** (2), 43–56.

Vázquez, I., Rodriguez-Iglesias, J., Maranon, E., Castrillon, L. & Alvarez, M. 2007 Removal of residual phenols from coke wastewater by adsorption. *Journal of Hazardous Materials* **147** (1–2), 395–400.

Villegas, L. G. C., Mashhadi, N., Chen, M., Mukherjee, D., Taylor, K. E. & Biswas, N. 2016 A short review of techniques for phenol removal from wastewater. *Current Pollution Reports* **2** (3), 157–167.

Wang, S. & Peng, Y. 2010 Natural zeolites as effective adsorbents in water and wastewater treatment. *Chemical Engineering Journal* **156** (1), 11–24.

Wang, W., Qiao, Y., Li, T., Liu, S., Zhou, J., Yao, H., Yang, H. & Xu, M. 2017 Improved removal of Cr(VI) from aqueous solution using zeolite synthesized from coal fly ash via mechano-chemical treatment. *Asia-Pacific Journal of Chemical Engineering* **12** (2), 259–267.

Yousef, R. I., El-Eswed, B. & Ala'a, H. 2011 Adsorption characteristics of natural zeolites as solid adsorbents for phenol removal from aqueous solutions: Kinetics, mechanism, and thermodynamics studies. *Chemical Engineering Journal* **171** (3), 1143–1149.

Yuwei, C. & Jianlong, W. 2011 Preparation and characterization of magnetic chitosan nanoparticles and its application for Cu(II) removal. *Chemical Engineering Journal* **168** (1), 286–292.

Zhou, L., Wang, Y., Liu, Z. & Huang, Q. 2009 Characteristics of equilibrium, kinetics studies for adsorption of Hg(II), Cu(II), and Ni(II) ions by thiourea-modified magnetic chitosan microspheres. *Journal of Hazardous Materials* **161** (2–3), 995–1002.

First received 5 February 2019; accepted in revised form 22 June 2019. Available online 5 August 2019